JAST, Vol. 14, No. 1, pp. 83-90

JAST
Journal of Aerospace Science and Technology

Science Article

A theoretical analysis of the influence of winding patterns on buckling load of filament wound composite pipes

Bahram Ghorbani Rezaei[1], Jafar EskandariJam[2]*
1 Department of mechanical engineering, Babol university of technology , Babol
2 – composite material and technology center, Tehran
Email: * **bahramghr@gmail.com**

While the composite pipes and cylinders manufacture by filament wound system, there are a lot of parameters that influence on the strength and mechanical behavior of them. This various mechanical behavior causes various buckling behavior. One of the most important parameters is winding pattern that have effects on critical buckling loads. So this parameter should be controlled since it effects on mechanical behavior of pipes and cylinders. In the present work the influence of winding patterns on the critical buckling load of filament wound pipes exposed by pure axial loading have been studied. The studied specimens are Glass/Epoxy tubes with [+55,-55]$_6$ lay-up(diameter to thickness ratio d/t of 10 and length of 280mm). Parameters were all considered to be consistent to investigate the effects of winding patterns there is just difference in winding pattern between three the experimental specimens. The lay-up is the result of classical theories. Love model and Galerkin's method were used to provide buckling equations and solve theoretically the resulted equation respectively. Although the results illustrate that there is a difference, about 2-4 percent, in terms of critical buckling load between disparate winding patterns, 16 unit cells winding pattern bears higher buckling load than other patterns. Also the results show that no evident patterns influence on buckling modes of pipes. Later, the maximum lateral buckling loads of the patterns are verified with experimental data.

Keywords: *Buckling-Glass/epoxy-winding pattern-Galerkin's method-parameters.*

Introduction

In recent years, the application of fiber-reinforced composite laminates has increased in various industrial
Structures(e.g. piping and vessels) due to their high stiffness and strength-to-weight ratios and the increase of shells properties by properly choosing the winding patterns to satisfy the desired performances. The study of effect of impressive parameters on mechanical behavior and buckling load has attracted the attention of many researchers.
In ref. [1] the influence of parameters (e.g. the tow tension) on the parameters (e.g. winding bandwidth) has been studied. Cohen [2] used the design of experiment method to recognize the applied tow tension during winding (winding tension) to be the most important manufacturing parameter for the resulting mechanical properties. Increasing this parameter caused a higher fiber volume fraction and it's a reason to increased strength of the filament wound pressure vessels.

1 Ph.D. student
2 Professor (Corresponding Author)

Received: 09 Oct. 2021
Accepted: 28 Oct. 2021

P.Martiny et l. 2002,[3] investigated the effect of filament winding tension on physical and mechanical properties of glass-fiber reinforced polymeric composites tubular. Their experimental results show that Under fiber-dominated loading conditions, higher winding tension leads to an improved resistance against failure of tubular components, whereas under matrix-dominated loading failure is delayed by reduced fiber tensioning. The effect of winding patterns on buckling load of cylinders are studied by H-Hernandez et l. in 2007,[4]. They are considered thin and thick cylinders (diameter to thickness ratio d/h=25 and 10 respectively) that exposed to external pressure. The experimental results of their paper has been shown that winding patterns have a negligible effect on buckling load. A Gharib et.al 2010 [5] used a genetic algorithm and neural network models to find the maximum fundamental frequency and critical buckling load, simultaneously. Their study was performed for the shell geometry with different sets of thickness to radius and length to radius ratios.

In this paper, results from an experimental study are presented [6]. The purpose is to investigate the influence of the winding patterns on the critical buckling load on tubular components. In this study lay-up of [+55,-55]6 was chosen, which is common in composite structures such as piping. This lay-up governing from classical theories. The investigation on mechanical properties was then extended to the critical buckling load of structures by using Love-type model and Galerkin's method respectively. The boundary condition was simply supported and the applied load was pure axial.

Verification of theoretical model

Cylinders are produced are made of the helical-winding pattern. The lay-up is [+55/-55]6 and 3 patterns of 8, 16 and 46 unit cells are made respectively. with length, inner radius and the thickness of 280mm, 30mm and 4.5mm respectively [6].

Three different patterns considered namely C8, C16, C46, with degree of interweaving of, respectively, 8, 16, and 46%.The unit cells of these structures are presented in Fig. 1 (the patterns are shown with a 450 winding angle instead of 550). The details of process is shown in [6]

The volume fraction of fiber and void has shown in table 1. The elastic properties of the tubes has shown in Table 2.

Table1: fiber and void volume fracture and weight of each pattern

Winding patterns	Void Fraction %	Fiber volume fraction%	Fiber weight fraction%	Density
C_8	2.26	69.70	81.07	2.097
C_{16}	1.97	69.74	80.92	2.101
C_{46}	2.50	69.80	81.33	2.096

Table 2: Mechanical properties of patterns

Winding patterns	E_{11}(Gpa)	E_{22}(Gpa)	ν_{12}
C_8	24.1	34.5	0.30
C_{16}	24	34.2	0.32
C_{46}	24.3	34.9	0.31

For each pattern the stiffness matrix (Q), was obtained using formula below:

$$Q_{11}=\frac{E_{11}}{1-\upsilon_{12}\upsilon_{21}}$$

$$Q_{12}=\frac{\upsilon_{12}E_2}{1-\upsilon_{12}\upsilon_{21}} \qquad (1)$$

$$Q_{22}=\frac{E_2}{1-\upsilon_{12}\upsilon_{21}}$$

$$Q_{66}=G_{12}$$

And the transformed reduced stiffness matrix $\overline{Q}$, was illustrated as:

$$\begin{aligned}
&\overline{Q}_{11}=Q_{11}.\cos(\theta)^4+Q_{22}.\sin(\theta)^4+\\
&2.(Q_{12}+2.Q_{66}).\sin(\theta)^2.\cos(\theta)^2\\
&\overline{Q}_{12}=(Q_{11}+Q_{22}-4.Q_{66}).\sin(\theta)^2\\
&.\cos(\theta)^2+Q_{12}\,(\cos(\theta)^4+\sin(\theta)^4)\\
&\overline{Q}_{22}=Q_{11}.\sin(\theta)^4+Q_{22}.\cos(\theta)^4+\\
&2(Q_{12}+2Q_{66}).\sin(\theta)^2.\cos(\theta)^2\\
&\overline{Q}_{16}=(Q_{11}-Q_{12}-2Q_{66}).\sin(\theta).\cos(\theta)^3-\\
&(Q_{22}-Q_{12}-2Q_{66}).\sin(\theta)^3.\cos(\theta)\\
&\overline{Q}_{26}=(Q_{11}-Q_{12}-2Q_{66}).\sin(\theta)^3.\cos(\theta)\\
&-(Q_{22}-Q_{12}-2Q_{66}).\sin(\theta).\cos(\theta)^3\\
&\overline{Q}_{66}=(Q_{11}+Q_{22}-2Q_{12}-2Q_{66}).\\
&\sin(\theta)2.\cos(\theta)^2+Q_{66}.(\sin(\theta)^4+\cos(\theta)^4
\end{aligned} \qquad (2)$$

The results of stiffness matrix, reduced stiffness matrix are shown in table 3 and 4 respectively.

Table 3. Stiffness matrix for each pattern(Gpa)

	Q_{11}	Q_{12}	Q_{13}	Q_{21}	Q_{22}	Q_{23}	Q_{31}	Q_{32}	Q_{33}
C_8	28.0	12.9	0	12.9	40.3	0	0	0	8.18
C_{16}	28.1	12.8	0	12.8	40.0	0	0	0	9.09
C_{46}	28.1	12.5	0	12.5	40.4	0	0	0	8.40

Table 4: reduced stiffness matrix for laminas(Gpa)

+55	$\bar{Q}_{11}$	$\bar{Q}_{12}$	$\bar{Q}_{13}$	$\bar{Q}_{21}$	$\bar{Q}_{22}$	$\bar{Q}_{23}$	$\bar{Q}_{31}$	$\bar{Q}_{32}$	$\bar{Q}_{33}$
C_8	33	14.2	-3.6	14.2	29	-1.9	-3.6	-1.9	10.5
C_{16}	34	14.1	-3.3	14.1	31	-2.3	-3.3	-2.3	10.4
C_{46}	32	14.7	-3.8	14.7	30	-2.0	-3.8	-2.0	10.6
-55									
C_8	33	14.2	3.6	14.2	29	1.9	3.67	1.94	10.56
C_{16}	35	14.17	3.30	14.17	31	2.3	3.30	2.31	10.44
C_{46}	32	14.74	3.68	14.74	30	2.0	3.87	2.09	10.60

A,B,D matrix expressed as equation 3:

$$(A_{ij}, B_{ij}, D_{ij}) = \sum_{k=1}^{n} \overline{Q_{ij}} [(t_{k+1} - t_k), (t_{k+1}^2 - t_k^2)/2, (t_{k+1}^3 - t_k^3)/3] \qquad (3)$$

In this equation Aij, Bij and Dij are extensional stiffness, bending-stretching coupling and flexural stiffness respectively. In this equations t is the thickness of each layer and i,j=1, 2, 3 and n is number of layers.$\bar{Q}$ij is transformed reduced stiffness matrix obtained from equation 2. The results of Aij, Bij and Dij components has shown in table 5 for each pattern.

Governing equations:

In the classical shell theory, the displacements of a point are assumed to have the form:

$$u = u(x,\theta,z) = u_0(x,\theta) + r\beta_x(x,\theta)$$
$$v = v(x,\theta,z) = v_0(x,\theta) + r\beta_\theta(x,\theta) \qquad (4)$$
$$w = w(x,\theta)$$

In the above u, v and w are displacements in x, θ and r direction respectively. U_0, v_0 and w are mid-plane displacements. β_x and β_θ are the rotation angles with respect to x and θ coordinate.
The mid-plane strains and curvatures are defined by:

$$\varepsilon_x^0 = \frac{\partial u_0}{\partial x} \qquad \beta_x = -\frac{\partial^2 w}{\partial x^2}$$
$$\varepsilon_\theta^0 = \frac{\partial v_0}{a\partial\theta} - \frac{w}{a} \qquad \beta_\theta = -\frac{1}{a^2}\left(\frac{\partial v_0}{\partial\theta} + \frac{\partial^2 w}{\partial\theta^2}\right) \qquad (5)$$
$$\gamma_s^0 = \frac{\partial u_0}{a\partial\theta} + \frac{\partial v_0}{\partial x} \qquad \beta_s = -\frac{2}{a}\left(\frac{\partial v_0}{\partial x} + \frac{\partial^2 w}{\partial x \partial\theta}\right)$$

Table 5: A, B and D component

Patterns Gpa.mm	A_{11}	A_{12}	A_{13}	A_{21}	A_{22}	A_{23}	A_{31}	A_{32}	A_{33}
C_8	0	0	0	0	0	32.43	0	32.43	0
C_{16}	0	0	0	0	0	29.13	0	29.13	0
C_{46}	0	0	0	0	0	36.82	0	36.82	0
Gpa Mm^2	B_{11}	B_{12}	B_{13}	B_{21}	B_{22}	B_{23}	B_{31}	B_{32}	B_{33}
C_8	211.0	90.39	6.33	90.39	185.13	2093	6.33	2093	66.9
C_{16}	197.8	80.69	5.69	80.69	174.6	2240.1	5.69	2240	59.4
C_{46}	228.7	98.48	6.67	98.48	200.65	2376.3	6.67	2376	70.8
Gpa Mm^3	D_{11}	D_{12}	D_{13}	D_{21}	D_{22}	D_{23}	D_{31}	D_{32}	D_{33}
C_8	6811	2917	204.5	2917	5975	33841	204	33841	2160
C_{16}	19162	7813	551	78.13	16910	108640	551	108640	5760
C_{46}	22148	9535	646.7	9535	19428	115528	646	115258	6857

The reference coordinate system for this model is presented in Figure 2.
To satisfy simply supported boundary conditions for buckling deformation we assumed solution in the form of:

$$u_0 = A\cos(\frac{m\pi x}{L}).\sin(n\theta)$$
$$v_0 = B\sin(\frac{m\pi x}{L}).\cos(n\theta) \quad (6)$$
$$w = C\sin(\frac{m\pi x}{L}).\sin(n\theta)$$

A, B and C are unknown constant, m and 2n are axial and circumferential half-waves numbers respectively.
Equilibrium equations for uniaxial compression have been written in final step. Subscript 1 refers to change value during the buckling [7].

$$\frac{\partial N_{x1}}{\partial x}+\frac{1}{a}\frac{\partial N_{x\theta 1}}{\partial \theta}=0$$
$$\frac{1}{a}\frac{\partial N_{\theta 1}}{\partial \theta}+\frac{\partial N_{x\theta 1}}{\partial x}-\frac{1}{a}\frac{\partial M_{x\theta 1}}{\partial x}+\frac{1}{a^2}\frac{\partial M\theta_1}{\partial \theta}+N_{x0}\frac{\partial^2 v_{01}}{\partial x^2}=0 \quad (7)$$
$$\frac{\partial^2 M_{x1}}{\partial x^2}+\frac{2}{a}\frac{\partial^2 M_{x\theta 1}}{\partial x\partial \theta}+\frac{1}{a^2}\frac{\partial^2 M_{\theta 1}}{\partial \theta^2}+\frac{N_{\theta 1}}{a}+N_{x0}\frac{\partial^2 w_1}{\partial x^2}=0$$

The subscript s refer to in-plane shear of x and ɵ plane. According to Love-type transfer shear deformation for $\frac{h}{a}<1$ is negligible. It means $r_{xr}=r_{\theta r}=0$
The buckling equations seek from 1, 2 and 3 equations and Love-type model. They are written in form of:

$$\begin{bmatrix} k_{11} & k_{12} & k_{13} \\ k_{21} & k_{22} & k_{23} \\ k_{31} & k_{32} & k_{33} \end{bmatrix}\begin{bmatrix} u_0 \\ v_0 \\ w \end{bmatrix}=\begin{bmatrix} 0 \\ 0 \\ 0 \end{bmatrix} \quad (8)$$

Each component of K matrix has a particular definition. K matrix has been written in .

Galerkin's method:

Equation 6 is zero due to boundary conditions. It has to be zero at each point of cylinder. The Galerkin's mathematics law expresses that:

$$\int_v \delta U^T K U dv=0 \quad (9)$$

$$\delta U^T=(\delta u_0,\delta v_0,\delta w)$$

We seek following equation after obtain the integral:
T matrix is defined by:
After solving equations above seek the solution in form of:

$$\text{Det}(T)=0 \quad (10)$$

That T is a matrix. Each of components of T matrix are expressed as:

$$T_{11}=A_{11}.(m\pi/L)^2+A_{33}.(n/a)^2$$
$$T_{12}=(A_{12}+A_{13}).(m\pi/L).(n/a)-(L/a).(B_{12}+2.B_{33}).(m.\pi/L).(n/a) \quad (11)$$
$$T_{13}=(A12/a).(m\pi/L)-B_{11}(m\pi/L)^3-B_{12}(m\pi/L)(n/a)^2-2.B_{33}.(m\pi/l).(n/a)^2$$
$$T_{21}=(A_{12}+A_{33}).(m\pi/L)(n/a)-(1/a).(B_{12}+B_{33}).(m\pi/L)(n/a)$$
$$T_{22}=A_{22}(n/a)^2+A_{33}(m\pi/L)^2-(2B_{22}/a)(n/a)^2-(3.B_{33}/a)(m\pi/L)^2+2(D_{33}/a^2)(m\pi/L)^2+(D_{22}/a^2).(n/a)^2+N_{x0}(m\pi/L)^2$$
$$T_{23}=(A_{22}/a)(n/a)-(B_{12}+2B_{33})(m\pi/L)^2(n/a)-B_{22}(n/a)^3-(B_{22}/a^2)(n/a)+(1/a)(2D_{33}+D_{12})(m\pi/L)^2.(n/a)+(D_{22}/a).(n/a)^3$$
$$T_{31}=T_{13}$$
$$T_{32}=(A_{22}/a)(n/a)-(B_{12}+2B_{33}).(m\pi/L)^2(n/a)-B_{22}(n/a)^3-(B_{22}/a^2)(n/a)+(1/a)(4D_{33}+D_{12})(m\pi/L)^2(n/a)+(D_{22}/a)(n/a)^3$$
$$T_{33}=(A_{22}/a^2)-(2B_{22}/a)(n/a)^2-(2B_{12}/a)(m\pi/L)^2+D_{11}(m\pi/L)^4+D_{22}(n/a)^4+(2D_{12}+4D_{33})(m\pi/L)^2(n/a)^2+N_{x0}.(m\pi/L)^2$$

Results

After solving the equation (10), Results of this equation provides in table 6. In this table for each of patterns observe critical buckling load and buckling moods. This table shows moods and buckling loads up to third moods. After third mood the results are very big and they can't be critical buckling loads. N_{xc} is the critical buckling load.

Table 6: result of buckling load

pattern	C_8	C_{16}	C_{46}	(m,n)
N_{xc}(Mpa)	765.4	791.2	765.4	(1,1)

In fig 3. The axial and circumferential moods have shown.

Conclusion

Table 1 shows the results of equation(7).Second pattern has shown greater buckling load in compared with the other patterns. Compared to third pattern, second pattern almost shows 4 percent resist on buckling load. This pattern also shows 2 percent resist on buckling load in compared with first pattern. Buckling moods were same for each pattern.

This study confirms results of [4]. In this study cylinders were under external pressure and the experimental results In this paper had shown that winding patterns have a negligible effect on buckling loads. The maximum difference between each patterns in this study is 7 percent. Also in this paper buckling moods appears on first and third for axial and circumferential respectively.

$$k_{21}() = \frac{A_{23}}{a^2}\frac{\partial^2}{\partial\theta^2}() - \frac{B_{12}}{a^2}\frac{\partial^2}{\partial x.\partial\theta}() - \frac{B_{13}}{a}\frac{\partial^2}{\partial x^2}() - \frac{B_{33}}{a^2}\frac{\partial^2}{\partial x.\partial\theta}() - \frac{B_{23}}{a^3}\frac{\partial^2}{\partial\theta^2}()$$

$$k_{22}() = \frac{2A_{23}}{a}\frac{\partial^2}{\partial x.\partial\theta}() - \frac{2B_{22}}{a^3}\frac{\partial^2}{\partial\theta^2}() - \frac{5B_{23}}{a^2}\frac{\partial^2}{\partial x.\partial\theta}() - \frac{3B_{13}}{a}\frac{\partial^2}{\partial x^2}() + \frac{3D_{23}}{a^3}\frac{\partial^2}{\partial x.\partial\theta}() + \frac{D_{22}}{a^4}\frac{\partial^2}{\partial\theta^2}() + \frac{2D_{33}}{a^2}\frac{\partial^2}{\partial x^2}() + N_{x0}\frac{\partial^2}{\partial x^2}()$$

$$k_{23} = -\frac{A_{23}}{a}\frac{\partial}{\partial x}() - \frac{B_{12}}{a}\frac{\partial^3}{\partial x^2.\partial\theta} - B_{13}\frac{\partial^3}{\partial x^3} - \frac{3B_{23}}{a^2}\frac{\partial^3}{\partial\theta^2.\partial x} - \frac{B_{22}}{a^3}\frac{\partial^3}{\partial\theta^3} - \frac{2B_{33}}{a}\frac{\partial^3}{\partial\theta.\partial x^2} + \frac{2B_{23}}{a^2}\frac{\partial}{\partial x} + \frac{B_{22}}{a^3}\frac{\partial}{\partial\theta} + \frac{3D_{23}}{a^3}\frac{\partial^3}{\partial x.\partial\theta^2} + \frac{D_{13}}{a}\frac{\partial^3}{\partial x^3} + \frac{D_{12}}{a^2}\frac{\partial^3}{\partial x^2.\partial\theta} + \frac{2D_{33}}{a^2}\frac{\partial^3}{\partial x^2.\partial\theta} + \frac{D_{22}}{a^4}\frac{\partial^3}{\partial\theta^3}$$

$$k_{31} = -k_{13}$$

$$k_{32} = \frac{A_{23}}{a}\frac{\partial}{\partial x} + \frac{B_{12}}{a}\frac{\partial^3}{\partial x^2.\partial\theta} + B_{13}\frac{\partial^3}{\partial x^3} + \frac{3B_{23}}{a^2}\frac{\partial^3}{\partial x.\partial\theta^2} + \frac{B_{22}}{a^3}\frac{\partial^3}{\partial\theta^3} + \frac{2B_{33}}{a}\frac{\partial^3}{\partial x^2.\partial\theta} - \frac{B_{22}}{a^3}\frac{\partial}{\partial\theta} - \frac{2B_{23}}{a^2}\frac{\partial}{\partial x} - \frac{D_{12}}{a^2}\frac{\partial^3}{\partial x^2.\partial\theta} - \frac{2D_{13}}{a}\frac{\partial^3}{\partial x^3} - \frac{4D_{23}}{a^3}\frac{\partial^3}{\partial x.\partial\theta^2} - \frac{D_{22}}{a^4}\frac{\partial^3}{\partial\theta^3} - \frac{4D_{33}}{a^2}\frac{\partial^3}{\partial x^2.\partial\theta}$$

$$k_{33} = -\frac{2B_{22}}{a^3}\frac{\partial^2}{\partial\theta^2} - \frac{4B_{23}}{a^2}\frac{\partial^2}{\partial x.\partial\theta} - \frac{2B_{12}}{a}\frac{\partial^2}{\partial x^2} - D_{11}.\frac{\partial^4}{\partial x^4} - \frac{2D_{12}}{a^2}\frac{\partial^4}{\partial x^2.\partial\theta^2} - \frac{4D_{13}}{a}\frac{\partial^4}{\partial x^3.\partial\theta} - \frac{4D_{23}}{a^3}\frac{\partial^4}{\partial x.\partial\theta^3} - \frac{4D_{33}}{a^2}\frac{\partial^4}{\partial x^2.\partial\theta^2} - \frac{D_{22}}{a^4}\frac{\partial^4}{\partial\theta^4} + N_{x0}\frac{\partial^2}{\partial x^2}$$

Figures:

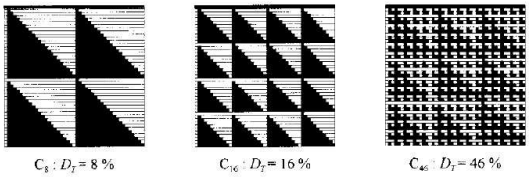

Fig. 1. Degree of weaving and unit cells of experimental structures.

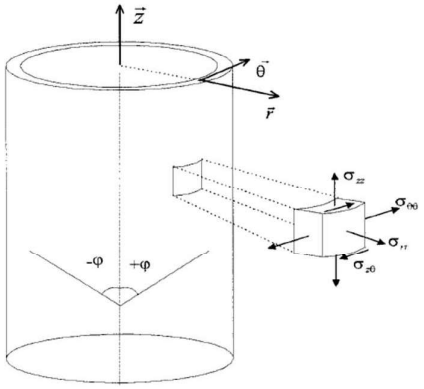

Fig 2: coordinate system

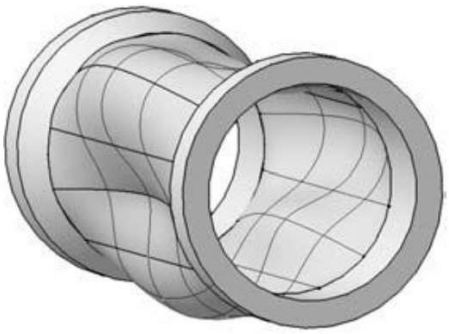

Fig 3: axial and circumferential moods

Refrences

1- Mertiny P, Ellyin F. Selection of optimal processing parameters in filament winding. In: Proceedings of 33rd International SAMPE Technical Conference. Seattle; November 2001. p. 1084–95.

2- Cohen D. Influence of filament winding parameters on composite vessel quality and strength. Composites Part A 1997;28A: 1035–47.

3- Mertiny P, Ellyin F. Influence of the filament winding tension on physical and mechanical properties of reinforced composites. Composites, Composites: Part A 33 (2002) 1615–1622.

4- H. Hernández-Morenoa, B. Douchin, F. Collombet, D. Choqueuse and P. Davies. Influence of winding pattern on the mechanical behavior of filament wound composite cylinders under external pressure. Composites Science and Technology. March 2008, volume 68, issue 3-4.

5- A.Gharib, M. Shakeri. Stacking sequence optimization of laminated cylindrical shells for buckling and free vibration

using genetic algorithm and neural networks. second International Conference on Engineering Optimization. September 6 - 9, 2010, Lisbon, Portugal.
6- J. Rousseau, D. Perreux, N. Verdiere, The influence of winding patterns on the damage behavior of filament-wound pipes, Composites Science and Technology 59 (1999) 1439±1449, 1998.